

Phoretic self-propulsion of Janus discs in the fast-reaction limit

Ehud Yariv

Department of Mathematics, Technion — Israel Institute of Technology, Haifa 32000, Israel

Darren Crowdy

Department of Mathematics, Imperial College London, London SW7 2AZ, UK

(Dated: October 12, 2020)

Abstract

Due to net interfacial consumption of solute, the two-dimensional problem of phoretic swimming is ill-posed in the standard description of diffusive transport, where the solute concentration satisfies Laplace’s equation. It becomes well-posed when solute advection is accounted for. We consider here the case of weak advection, where solute transport is analyzed using matched asymptotic expansions in two separate asymptotic regions, a near-field region in the vicinity of the swimmer and a far-field region where solute advection enters the dominant balance. We carry out the analysis for a standard Janus configuration, where half of the particle boundary is active and the other half is inert. Our main focus lies in the limit of fast reaction, which leads to a mixed boundary-value problem in the near field. That problem is solved using conformal mapping techniques. Our asymptotic scheme furnishes the following implicit equation for the particle velocity s in the direction of the active portion of its boundary,

$$2s \left(8 \ln \frac{8D}{|s|a} - \gamma \right) = \frac{bc_\infty}{a},$$

wherein a is the particle radius, D the solute diffusivity, c_∞ its far-field concentration, b the diffusio-osmotic slip coefficient, and γ the Euler–Mascheroni constant. The nonlinear dependence of s upon bc_∞ is a signature of the non-vanishing effect of solute advection.

11 I. INTRODUCTION

12 Self-propelled “swimmers” have been natural candidates for idealized two-dimensional
13 investigations [1]: being force-free, no “Stokes paradox” arises when addressing the relevant
14 limit of inertia-free flow. It is desirable [2] to employ similar two-dimensional models to
15 analyze phoretic swimmers, which propel through a liquid solution by a chemical reaction
16 on their boundary [3]. When considering phoretic swimmers, however, the net consumption
17 of solute implies that the two-dimensional version of the standard continuum description is
18 ill-posed. In that description, the (presumably diffusive) transport of solute is described by
19 Laplace’s equation; in two dimensions, this equation gives rise to a sink term that diverges
20 logarithmically at large distances. Thus, while the flow problem does not introduce any
21 conceptual difficulties, it is the underlying solute-transport problem that poses a non-trivial
22 obstacle [4].

23 To circumvent this obstacle Crowdy [5] analyzed a two-dimensional Janus particle with
24 two faces having different surface activities, absorbing and emitting solute in such a way
25 that there is no net source production. While this situation is not generic, it turns out to
26 be a theoretically important case study because the steady velocity of the particle in an
27 unbounded solution can be found in closed form, as can the dynamical system governing its
28 unsteady motion near a no-slip wall [5].

29 Naturally, it is of interest to study the general case where the particle is a net source
30 of solute. Sondak *et al.* [4] noted that allowing for solute advection results in a well-
31 posed problem even when there is a net production of solute. It follows that the closest
32 two-dimensional well-posed analog of the three-dimensional diffusive transport is provided
33 by the asymptotic limit of weak (but non-vanishing) advection. This singular limit was
34 addressed by Yariv [6] using matched asymptotic expansions. Thus, the transport of solute
35 was calculated in two different asymptotic regions: one on the scale of the particle, where
36 solute is transported diffusively, and one on a remote scale, where advection enters the
37 leading-order balance. A key difference between that asymptotic analysis and comparable
38 classical analyses of transport phenomena [7] is that the velocity field is not externally
39 imposed but is rather set by the interfacial solute gradients at the particle boundary. This
40 results in a non-standard coupling (above and beyond that of asymptotic matching) between
41 the solutions in the two asymptotic regions.

42 In Yariv’s scheme [6], the solute concentration on the particle scale has been expanded
43 using two-dimensional multipoles of Laplace’s equation. The coefficients of this expansion
44 are set by the appropriate model of interfacial solute production. Following Michelin &
45 Lauga [8], Yariv [6] used first-order kinetics, where the relative magnitude of interfacial
46 reaction is specified by the Damköhler number. The associated boundary condition then
47 results in an indeterminate linear system governing the coefficients; asymptotic matching
48 with the remote region eventually provides a determinate system, which may be solved for
49 any value of the Damköhler number.

50 Following realistic applications, typical interest lies in the “canonical” Janus-particle con-
51 figuration, where the particle boundary consists of two homogenous portions — one inert
52 and one active. For this configuration, the methodology used by Yariv [6] is inappropriate in
53 the fast reaction limit. In that limit, where the Damköhler number becomes large, the solute
54 concentration satisfies a mixed boundary-value problem, governed by a Neumann condition
55 on the inert portion of the boundary and a Dirichlet condition on the active portion. Such
56 a mixed problem does not readily provide algebraic equations for the coefficients in a mul-
57 tipole expansion. This failure may be attributed to the singular nature of the fast reaction
58 limit: indeed, mixed boundary-value problems are known [9] to exhibit square-root-type
59 singularities at the points of transition between the different types of boundary conditions.

60 On the other hand, it turns out that the mixed boundary-value problem which emerges
61 in that very limit may be naturally handled using conformal mapping techniques, similar
62 to those which have been applied to analyze longitudinal flows about superhydrophobic
63 surfaces [10]. The goal of the present paper is to revisit the two-dimensional autophoresis
64 problem with a view towards the fast-reaction limit, which is known to be relevant to realistic
65 experiments [11]. In contrast to the generic analysis of Yariv [6], which allows for arbitrary
66 distributions of interfacial kinetics, we focus here upon the Janus configuration from the
67 outset.

68 II. PHYSICAL PROBLEM

69 A chemically reactive circular particle (radius a) is freely suspended in an unbounded
70 solution (solute diffusivity D). The reference solute concentration, at large distances from
71 the particle, is denoted by c_∞ . We assume a Janus configurations, where half of the particle

72 boundary is chemically active while the other half is chemically inert. On the active portion,
 73 solute transfer is modeled using a first-order chemical reaction [8, 11],

$$\text{solute absorption (per unit area)} = k \times \text{local value of solute concentration}, \quad (2.1)$$

74 where the (presumably uniform) rate constant k is positive.

75 On the macroscale, the short-range interaction between the solute molecules and the
 76 particle is manifested by diffusio-osmotic slip [12],

$$\text{slip velocity} = b \times \text{surface gradient of solute concentration}. \quad (2.2)$$

77 Following the common practice [4, 8], we assume that b is uniform. Note that b is a signed
 78 quantity, positive for repulsive interactions and negative for attractive ones. The velocity
 79 scale associated with (2.2) is $\mathcal{U} = |b|c_\infty/a$. Defining the intrinsic Péclet number Pe as $a\mathcal{U}/D$
 80 thus gives

$$\text{Pe} = \frac{|b|c_\infty}{D}. \quad (2.3)$$

81 It follows from the problem symmetry that the force-free particle reacts by moving along
 82 its symmetry diameter with a constant velocity, say s (defined positive when the particle
 83 propagates in the direction of its active cap). By not rotating, the torque-free condition is
 84 trivially satisfied. Our goal is the determination of s .

85 III. DIMENSIONLESS FORMULATION

86 We employ a dimensionless notation where all length variables are normalized by a .
 87 The analysis is carried out in a particle-fixed reference system with origin at the particle
 88 center. In that system we use the (x, y) Cartesian coordinates, defined such that the x -
 89 axis is aligned along the symmetry diameter of the particle, pointing in the direction of
 90 the active cap. We additionally utilize the (r, θ) polar coordinates, with θ measured in
 91 the counterclockwise direction from the x -axis. In what follows we consider the coupled
 92 transport–flow problem governing the solute concentration c , normalized by c_∞ , and fluid
 93 velocity \mathbf{u} , normalized by \mathcal{U} . Our interest is in the velocity $U(= s/\mathcal{U})$ of the particle
 94 relative to the otherwise quiescent liquid; in the particle-fixed reference frame this velocity
 95 is manifested as the uniform streaming $-U\hat{\mathbf{i}}$ at infinity, $\hat{\mathbf{i}}$ being a unit vector in the x -
 96 direction.

97 The dimensionless solute transport problem is governed by: (i) the advection–diffusion
 98 equation,

$$\nabla^2 c = \text{Pe } \mathbf{u} \cdot \nabla c \quad \text{for } r > 1; \quad (3.1)$$

99 (ii) the kinetic condition at the particle boundary,

$$\frac{\partial c}{\partial r} = \begin{cases} \text{Da } c, & 0 < |\theta| < \pi/2 \\ 0, & \pi/2 < |\theta| < \pi \end{cases} \quad \text{at } r = 1, \quad (3.2)$$

100 where

$$\text{Da} = \frac{ak}{D} \quad (3.3)$$

101 is the Damköhler number, representing the ratio of diffusive (a^2/D) to reactive (a/k) time
 102 scales; and (iii) the approach to the reference concentration at large distances,

$$\lim_{r \rightarrow \infty} c = 1. \quad (3.4)$$

103 The flow is governed by: (i) the continuity and Stokes equations [the former tacitly
 104 employed in (3.1)]; (ii) diffusio-osmotic slip [cf. (2.2)]

$$\mathbf{u} = \hat{\mathbf{e}}_\theta M \frac{\partial c}{\partial \theta} \quad \text{at } r = 1, \quad (3.5)$$

105 where $M = b/|b|$; (iii) far-field approach to a uniform stream,

$$\lim_{r \rightarrow \infty} \mathbf{u} = -U \hat{\mathbf{z}}; \quad (3.6)$$

106 and (iv) the requirement that the particle is force-free. The latter, in conjunction with
 107 (3.5)–(3.6), provides the particle velocity as a quadrature [13],

$$U = \frac{M}{2\pi} \int_{-\pi}^{\pi} \frac{\partial c}{\partial \theta} \Big|_{r=1} \sin \theta \, d\theta. \quad (3.7)$$

108 The coupled flow–transport problem is described in Fig. 1. In principle, this nonlinear
 109 problem provides U as a function of Pe , Da and $M (= \pm 1)$. While (3.7) may appear to
 110 suggest that there is no need to solve for the flow, this is not the case due to the advective
 111 term in (3.1).

112 Relying upon the three-dimensional problem in the absence of advection, one may naïvely
 113 assume that

$$c \rightarrow c, \quad \mathbf{u} \rightarrow -\mathbf{u} \quad \text{under the transformation } M \rightarrow -M, \quad (3.8)$$

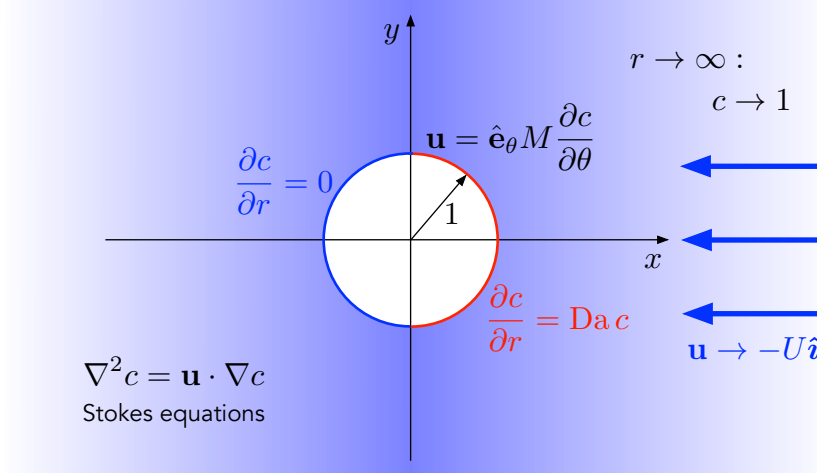


FIG. 1. The nonlinearly coupled boundary-value problem.

114 and, in particular,

$$U \rightarrow -U \quad \text{under the transformation} \quad M \rightarrow -M. \quad (3.9)$$

115 However, symmetry (3.8) is incompatible with (3.1) for all positive Pe . In general, the
 116 nonlinear dependence upon the flow carries out a non-trivial dependence upon M .

117 Regardless of the validity of (3.9), it is plausible that the sign of U coincides with that
 118 of M . Indeed, with condition (3.2) implying larger fluxes on the “right” face of the particle
 119 ($|\theta| < \pi/2$), and with the concentration being fixed at infinity by (3.4), it is anticipated that
 120 c is smaller on that face. The gradients of c are then expected to point to the “left” face of
 121 the particle, where c is larger. For positive M this is also the direction of slip [see (3.5)], so
 122 a force-free particle reacts by moving to to the right. [This is also evident from (3.7).] This
 123 suggests that:

$$U = M|U|. \quad (3.10)$$

124 IV. SMALL PÉCLET NUMBERS

125 For small Péclet numbers, the advection–diffusion equation (3.1) degenerates at leading
 126 order to Laplace’s equation:

$$\nabla^2 c = 0 \quad \text{for} \quad r > 1, \quad (4.1)$$

127 whereby coupling with the flow may seem to have disappeared. However, condition (3.2)
 128 implies that

$$\oint_{r=1} \frac{\partial c}{\partial r} d\theta > 0 \quad (= F, \text{ say}), \quad (4.2)$$

129 for all positive Da values. The associated net flux into the particle necessitates the asymp-
 130 totic behavior

$$c \sim \frac{F}{2\pi} \ln r \quad \text{for } r \gg 1, \quad (4.3)$$

131 which is incompatible with the decay condition (3.4). The limit of small Péclet numbers is
 132 a singular one.

133 It is of course well known [14] that small-Péclet-number problems are generically singular,
 134 becoming nonuniform at large distances. The non-uniformity in the present problem may be
 135 traced back to (4.3), which implies that ∇c decays as $1/r$ at large r . With that decay rate
 136 we find that the left- and right-hand sides of (3.1) are $O(r^{-2})$ and $O(\text{Pe} r^{-1})$, respectively;
 137 regardless of how small is Pe, advection always enters the leading-order balance at $r =$
 138 $O(\text{Pe}^{-1})$. Laplace’s equation (4.1) thus constitutes a leading-order approximation only on
 139 the particle-scale region, where $r = O(1)$. It needs to be supplemented by an additional
 140 “remote” expansion, valid at $r = O(\text{Pe}^{-1})$. With that approach, the logarithmic divergence
 141 in (4.3) is acceptable, as it is the remote expansion that needs to satisfy (3.4).

142 It is important to note that the flow is coupled to the solute concentration only through
 143 the slip condition (3.5). The flow problem is accordingly “unaware” of the scale separation
 144 in the solute-transport problem, and remains formulated on a single length scale. It follows
 145 that expression (3.7) for the particle velocity remains intact.

146 Since interest ultimately lies in that velocity, it may appear that it is sufficient to solve
 147 the particle-region transport, and then make use of (3.7). In the general case, however,
 148 such an independent analysis cannot be realized. Indeed, consider the refinement of the
 149 asymptotic behavior (4.3),

$$c \sim \frac{F}{2\pi} \ln r + G + O(r^{-1}) \quad \text{for } r \gg 1, \quad (4.4)$$

150 where G represents the “background” solute concentration, relative to that at infinity, and
 151 the $O(r^{-1})$ error represents decaying harmonics. Since condition (3.4) cannot be utilized in
 152 the particle-region analysis, it does not aid in determining F and G . It is then evident that
 153 condition (3.2) does not suffice to determine both F and G . Without asymptotic matching
 154 with the remote region, the particle-scale problem is indeterminate.

155 It is therefore necessary to analyze both the particle region and the remote region. The
 156 procedure we adopt is threefold: first, we solve the remote-region transport; second, we
 157 exploit that solution in conjunction with (4.4) to obtain a relation governing F , G and
 158 U from the requirement of asymptotic matching between the two regions; third, we solve
 159 the particle-region transport, treating F as given. The resulting expressions for G and U
 160 (as functions of F), in conjunction with the above relation, eventually furnish the particle
 161 velocity.

162 V. REMOTE-REGION ANALYSIS

163 The remote region is naturally analyzed using the stretched Cartesian coordinates (x', y') ,
 164 defined by

$$(x', y') = \text{Pe} (x, y). \quad (5.1)$$

165 Similarly, we define $r' = \text{Pe} r$. In the remote region we additionally employ the fields c' and
 166 \mathbf{u}' , functions of (x', y') , which are defined as

$$c' = c - 1, \quad \mathbf{u}' = \mathbf{u}. \quad (5.2)$$

167 We therefore obtain at leading order from (3.1)

$$\nabla'^2 c' = \mathbf{u}' \cdot \nabla' c', \quad (5.3)$$

168 where $\nabla' = \hat{\mathbf{i}} \partial / \partial x' + \hat{\mathbf{j}} \partial / \partial y'$ is the stretched gradient operator. This equation is subject to
 169 large- r' decay, which follows from (3.4).

170 Given the approach (3.6) to a uniform streaming velocity, it is evident that $\mathbf{u}' \equiv -\hat{\mathbf{i}}U$
 171 at leading order. Equation (5.3) is therefore simplified to $\nabla'^2 c' = -U \partial c' / \partial x'$. Substituting
 172 $c' = e^{-\frac{1}{2}Ux'} H$ we find that H satisfies the modified Helmholtz equation, $\nabla'^2 H = \frac{1}{4}U^2 H$.
 173 The solution of that equation that decays at infinity and is least singular at the origin is a
 174 radially symmetric screened source of magnitude D , $(D/2\pi)K_0(|U|r'/2)$, in which K_0 is the
 175 modified Bessel function of the second kind. We therefore obtain

$$c' = \frac{D}{2\pi} e^{-\frac{1}{2}Ux'} K_0 \left(\frac{|U|r'}{2} \right). \quad (5.4)$$

176 Using the small-argument behavior of K_0 [15] we find, with an algebraically small error,

$$c' \sim -\frac{D}{2\pi} \left(\ln \frac{|U|r'}{4} + \gamma \right) \quad \text{as } r' \rightarrow 0, \quad (5.5)$$

177 wherein γ is the Euler–Mascheroni constant. Asymptotic matching with (4.4) gives

$$F = -D, \quad G = 1 + \frac{D}{2\pi} \left(\ln \frac{4}{|U|\text{Pe}} - \gamma \right), \quad (5.6)$$

178 where, following the conventional approach [16], logarithmic terms are considered on par
179 with $O(1)$ terms as $\text{Pe} \rightarrow 0$. Combining (5.6) to eliminate D we obtain

$$G = 1 - \frac{F}{2\pi} \left(\ln \frac{4}{|U|\text{Pe}} - \gamma \right) \quad (5.7)$$

180 which provides the requisite extra condition for uniquely determining the particle-scale so-
181 lution. While the equations governing c are linear, condition (5.7) is nonlinear, representing
182 the non-vanishing signature of solute advection. Since Pe is small, it follows from (5.7) that
183 the signs of F and G are opposite; with F being positive [see (4.2)], the background solute
184 concentration G is negative, as could have been expected for an absorption process.

185 We now claim that at leading order, the symmetry (3.9) does hold. The proof consists
186 of three elements: (i) the particle-scale calculation of c (and in particular the relation it
187 imposes between F and G) is unaffected by the flow and hence by the sign of M ; (ii) The
188 calculation of U via (3.7) is compatible with (3.9); and (iii) the closure condition (5.7), which
189 serves to uniquely determine the inner problem, is also compatible with (3.9).

190 VI. THE PARTICLE-SCALE PROBLEM IN THE FAST REACTION LIMIT

191 The particle-scale solute-transport problem is governed by Laplace’s equation (4.1) and
192 the kinetic condition (3.2). The far-field condition (3.4) does not apply on that scale.
193 Instead, we impose the asymptotic condition (4.3), treating $F > 0$ as given. This results in
194 a well-posed problem (and excludes the trivial solution $c \equiv 0$)

Our interest lies in the limit $\text{Da} \rightarrow \infty$, where condition (3.2) is degenerated to the
following mixed Dirichlet–Neumann condition at $r = 1$:

$$c = 0 \quad \text{for} \quad 0 < |\theta| < \pi/2, \quad (6.1a)$$

$$\frac{\partial c}{\partial r} = 0 \quad \text{for} \quad \pi/2 < |\theta| < \pi. \quad (6.1b)$$

195 The problem governing c on the particle scale, associated with that condition, is described in
196 Fig. 2. This problem depends only upon (the yet unknown) flux F . In solving the particle-
197 scale problem, our goal is to obtain — in terms of F — both the constant G appearing in
198 (4.4) and the particle velocity U , as given by the quadrature (3.7).

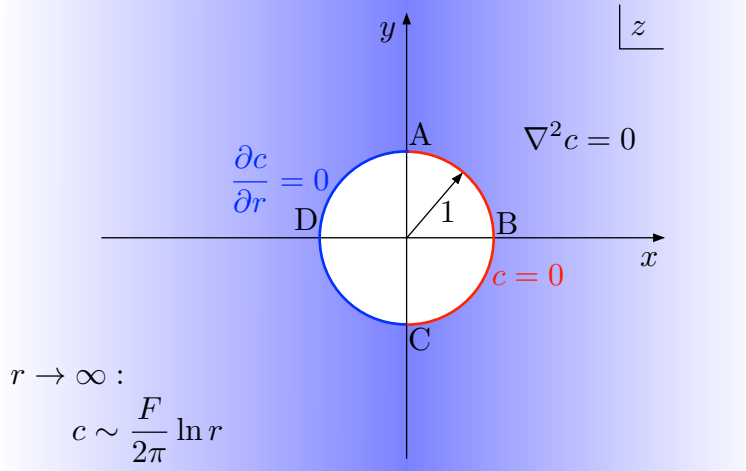


FIG. 2. The particle-scale transport problem in the fast-reaction limit.

200 Denoting the harmonic conjugate of c by ψ , we embed the concentration c in the complex
 201 potential Φ ,

$$\Phi = c + i\psi, \quad (6.2)$$

202 an analytic function of $z = x + iy$. Making use of the Cauchy–Riemann conditions we find
 203 that, in terms of Φ , the mixed condition (6.1) reads (refer to Fig. 2)

$$\operatorname{Re}\{\Phi\} = 0 \text{ on ADC}, \quad \operatorname{Im}\{\Phi\} = 0 \text{ on ABC}. \quad (6.3)$$

204 Also, in terms of Φ , the far-field asymptote (4.4) becomes

$$\Phi(z) \sim \frac{F}{2\pi} \log z + G + O(|z|^{-1}) \quad \text{for } |z| \gg 1. \quad (6.4)$$

205 Following Crowdy [10, 17, 18], we employ two conformal mappings (see Fig. 3) in terms
 206 of the parametric variable ζ . The first is

$$f(\zeta) = \frac{(\zeta - \bar{\alpha})(\zeta - 1/\bar{\alpha})}{(\zeta - \alpha)(\zeta - 1/\alpha)}, \quad (6.5)$$

207 where the point α is on the imaginary axis in the upper-half unit disc in the complex ζ -plane.
 208 This mapping transplants this semi-disc to the exterior of the unit circle with $\zeta = \alpha$ being
 209 mapped to infinity. Choosing

$$\alpha = i \tan(\pi/8), \quad (6.6)$$

210 which is derived by insisting that $f(1) = i$, the real diameter ABC ($-1 < \zeta < 1$) is mapped
 211 onto the right side of the unit circle while the upper-half unit circle CDA ($|\zeta| = 1, \operatorname{Im}\{\zeta\} > 0$)
 212 is mapped onto the respective left side.

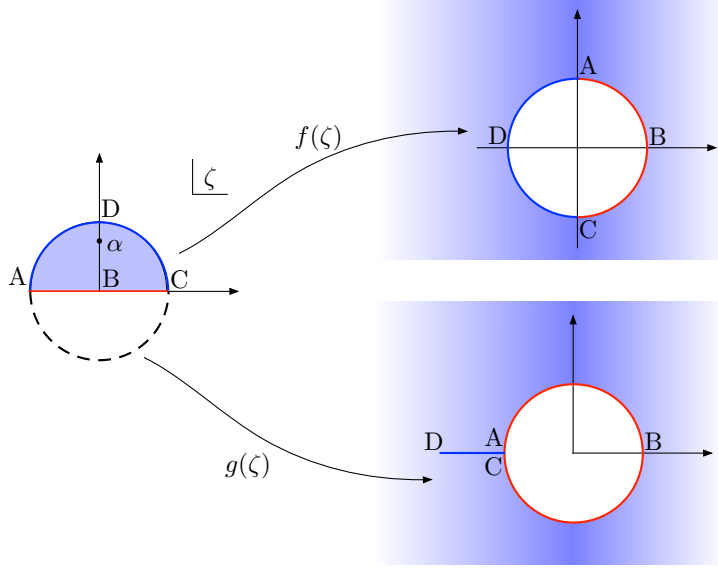


FIG. 3. The conformal map $f(\zeta)$ transplants the upper unit ζ disc to the unbounded region exterior to a unit disc. The conformal map $g(\zeta)$ transplants the upper unit ζ disc to the unbounded region exterior to a unit disc with a slit.

213 The second is the radial-slit mapping [10, 17, 18],

$$g(\zeta) = \frac{(\zeta - \bar{\alpha})(\zeta - 1/\alpha)}{(\zeta - \alpha)(\zeta - 1/\bar{\alpha})}, \quad (6.7)$$

214 which also sends the upper-half unit disc to the exterior of the unit circle. Now, however,
 215 the real diameter ABC is mapped onto the entire unit circle. The upper-half unit circle
 216 CDA is now mapped onto a finite slit which extends between -1 (points A and C) and
 217 $-(\sqrt{2} + 1)/(\sqrt{2} - 1)$ (point D).

218 We claim that the required solution for $\Phi(z)$ can be written down immediately in the
 219 parametric form

$$z = f(\zeta), \quad \Phi(z) = h(\zeta), \quad (6.8)$$

220 where

$$h(\zeta) = \frac{F}{2\pi} \log g(\zeta). \quad (6.9)$$

221 To prove the above claim we note, using the geometrical properties of the radial slit
 222 mapping $g(\zeta)$, that the real and imaginary parts of

$$h(\zeta) = \frac{F}{2\pi} \{ \ln |g(\zeta)| + i \arg g(\zeta) \} \quad (6.10)$$

223 respectively vanish on the unit circle ABC and the slit CDA in the transformed plane. Since
 224 homogeneous Dirichlet conditions are conformally invariant [19], it follows that conditions
 225 (6.3) are satisfied. Moreover, by considering f and g near the point α (where $z \rightarrow \infty$) we
 226 find that $g(\zeta) \sim 2z$. It then follows that

$$\Phi(z) \sim \frac{F}{2\pi} \log(2z), \quad (6.11)$$

227 consistent with the far-field requirement (4.3). Comparing with (4.4) we obtain

$$G = \frac{F}{2\pi} \ln 2. \quad (6.12)$$

228 It is possible to invert the mapping $z = f(\zeta)$ to find ζ , and hence $\Phi(z)$, explicitly as
 229 a function of z . The resulting expressions [17] make evident the presence of square root
 230 singularities at $z = \pm i$. To extend the solution form (6.8)–(6.9) to more general Janus
 231 particles with different coverage ratios requires merely altering the choice (6.6), as done in
 232 other studies [17].

233 Consider now the quadrature (3.7). Given condition (6.1a) on the right face of the
 234 particle, it now reads

$$U = \frac{M}{2\pi} \int_{\text{ADC}} \frac{\partial c}{\partial \theta} \sin \theta d\theta. \quad (6.13)$$

235 Using the Cauchy–Riemann conditions it is readily verified that

$$z\Phi'(z) = \frac{\partial c}{\partial r} - i \frac{\partial c}{\partial \theta}. \quad (6.14)$$

236 Since $\partial c/\partial r = 0$ at the left face ADC, we have there $\partial c/\partial \theta = iz\Phi'(z)$. Moreover, on the
 237 unit circle, where $z = e^{i\theta}$, $\sin \theta d\theta = -\text{Re}\{dz\}$. We conclude that

$$U = \frac{M}{2\pi} \text{Im} \int_{\text{ADC}} z\Phi'(z) dz. \quad (6.15)$$

238 Changing the integration variable to ζ using (6.8) we therefore obtain

$$U = \frac{M}{2\pi} \text{Im} \int_{\text{ADC}} f(\zeta)h'(\zeta) d\zeta. \quad (6.16)$$

239 It is a simple matter to confirm directly from (6.5), (6.7) and (6.9) that

$$f(1/\zeta) = f(\zeta), \quad h(1/\zeta) = -h(\zeta), \quad (6.17)$$

240 allowing to express U as an integral over the entire unit circle in the ζ -plane:

$$U = \frac{M}{4\pi} \text{Im} \int_{|\zeta|=1} f(\zeta)h'(\zeta) d\zeta, \quad (6.18)$$

241 where the integration is carried out in the clockwise direction. Substitution of (6.5), (6.7)
 242 and (6.9) reveals that the integrand is a rational function of ζ with a single (second-order)
 243 pole inside the unit circle, at $\zeta = \alpha$, with residue $-F/2\pi$. The residue theorem therefore
 244 gives

$$U = \frac{MF}{4\pi}. \quad (6.19)$$

245 VII. COMBINING THE RESULTS

246 Having derived relations (6.12) and (6.19), we have all that we need from the particle-
 247 scale analysis. Plugging these into the closure condition (5.7) and further assuming that
 248 (3.10) indeed holds, we eventually obtain the equation

$$2MU \left(\ln \frac{8}{MUPe} - \gamma \right) = 1, \quad (7.1)$$

249 which implicitly provides MU as a function of Pe . Since it results in a positive MU for
 250 $Pe \ll 1$, we have justified (3.10) *a posteriori*.

251 Note that the product MU constitutes the ratio of the dimensional velocity s to the
 252 signed velocity scale bc_∞/a , while the product $MUPe$ is equal to the Péclet number $|s|a/D$
 253 associated with particle motion (as opposed to the intrinsic number Pe). The dimensional
 254 counterpart of (7.1) is

$$2s \left(8 \ln \frac{8D}{|s|a} - \gamma \right) = \frac{bc_\infty}{a}. \quad (7.2)$$

255 This equation illustrates how the inverse scaling with particle size, pertinent in the three-
 256 dimensional version of the fast-reaction limit [11], breaks down in two dimensions.

257 VIII. CONCLUDING REMARKS

258 The present contribution, which is based upon a combination of singular perturbation
 259 analysis with conformal mapping techniques, complements the original two-dimensional
 260 analysis of Yariv [6], which is inadequate to handle the mixed boundary-value problem
 261 that emerges in the fast reaction limit.

262 We briefly comment upon the non-dimensionalization process. In his two-dimensional
 263 analysis, Yariv [6] followed Michelin & Lauga [8] in choosing the solute-concentration scale
 264 as one that estimates the perturbation from the reference concentration at infinity, rather

265 than that very concentration. Unsurprisingly, then, the resulting velocity scale ($\text{Da}\mathcal{U}$ in
266 the present notation) properly represents the small- Da limit, where the deviation from the
267 reference concentration is indeed a small perturbation. While that choice is also adequate
268 to analyze moderate Da numbers, it results in non-representative concentration and velocity
269 scales in the analysis of the large- Da limit. As a consequence, it has the unfortunate artifact
270 of a dimensionless particle velocity that diminishes as $\text{Da} \rightarrow \infty$. That is indeed evident
271 from Fig. 1 of Yariv [6].

272 In the present analysis, where we use the reference concentration and the associated
273 velocity scale \mathcal{U} , the problem formulation differs from that of Yariv [6]. In the large- Da
274 limit, the dimensionless particle velocity now attains a finite limit. The calculation of that
275 velocity has been the ultimate goal of the present analysis.

276 It is worth emphasizing that the present analysis made use of two limits, namely small Pe
277 and large Da . These two limits differ fundamentally, as the first is singular and the second
278 is regular; given this difference, there is no restriction upon the relative values of Pe and
279 $1/\text{Da}$. In particular, note that the discussion in Sec. IV and the subsequent remote-region
280 analysis in Sec. V are valid for all values of Da .

281 A natural followup of the present work is the analysis of the comparable three-dimensional
282 problem. As that problem is clearly well posed for zero Péclet numbers, no need arises for
283 the incorporation of weak advection. The major challenge in that followup is the mixed
284 boundary-value problem that arises at large Damköhler numbers. The particle speed at-
285 tained in that limit was obtained by Ebbens *et al.* [11] by extrapolating from speed val-
286 ues obtained numerically at finite values of Da . To the best of our knowledge, the mixed
287 boundary-value problem appropriate to the limit $\text{Da} \rightarrow \infty$ has never been solved directly.

288 [1] D. Crowdy and O. Samson, “Hydrodynamic bound states of a low-Reynolds-number swimmer
289 near a gap in a wall,” *J. Fluid Mech.* **667**, 309–335 (2011); A. M. J. Davis and D. G.
290 Crowdy, “Stresslet asymptotics for a treadmilling swimmer near a two-dimensional corner:
291 hydrodynamic bound states,” *Proc. Roy. Soc. London. A* **468**, 3765–3783 (2012); “Matched
292 asymptotics for a treadmilling low-Reynolds-number swimmer near a wall,” *Q. J. Mech. Appl.*
293 *Math.* **66**, 53–73 (2013).

- 294 [2] D. Boniface, C. Cottin-Bizonne, R. Kervil, C. Ybert, and F. Detcheverry, “Self-propulsion
295 of symmetric chemically active particles: Point-source model and experiments on camphor
296 disks,” *Phys. Rev. E* **99**, 062605 (2019); W.-F. Hu, T.-S. Lin, S. Rafai, and C. Misbah,
297 “Chaotic swimming of phoretic particles,” *Phys. Rev. Lett.* **123**, 238004 (2019).
- 298 [3] R. Golestanian, T. B. Liverpool, and A. Ajdari, “Designing phoretic micro-and nano-
299 swimmers,” *New J. Phys.* **9**, 126 (2007).
- 300 [4] D. Sondak, C. Hawley, S. Heng, R. Vinsonhaler, E. Lauga, and J.-L. Thiffeault, “Can phoretic
301 particles swim in two dimensions?” *Phys. Rev. E* **94**, 062606 (2016).
- 302 [5] D. G. Crowdy, “Wall effects on self-diffusiophoretic Janus particles: a theoretical study,” *J.*
303 *Fluid Mech.* **735**, 473–498 (2013).
- 304 [6] E. Yariv, “Two-dimensional phoretic swimmers: the singular weak-advection limits,” *J. Fluid*
305 *Mech.* **816**, R3 (2017).
- 306 [7] L. G. Leal, *Advanced Transport Phenomena: Fluid Mechanics and Convective Transport Pro-*
307 *cesses* (Cambridge University Press, New York, 2007).
- 308 [8] S. Michelin and E. Lauga, “Phoretic self-propulsion at finite Péclet numbers,” *J. Fluid Mech.*
309 **747**, 572–604 (2014).
- 310 [9] I. N. Sneddon, *Mixed Boundary Value Problems in Potential Theory* (Wiley, New York, 1966).
- 311 [10] D. G. Crowdy, “Frictional slip lengths for unidirectional superhydrophobic grooved surfaces,”
312 *Phys. Fluids* **23**, 072001 (2011).
- 313 [11] S. Ebbens, M.-H. Tu, J. R. Howse, and R. Golestanian, “Size dependence of the propulsion
314 velocity for catalytic Janus-sphere swimmers,” *Phys. Rev. E* **85**, 020401 (2012).
- 315 [12] J. L. Anderson, “Colloid transport by interfacial forces,” *Annu. Rev. Fluid Mech.* **30**, 139–165
316 (1989).
- 317 [13] T. M. Squires and M. Z. Bazant, “Breaking symmetries in induced-charge electro-osmosis and
318 electrophoresis,” *J. Fluid Mech.* **560**, 65–101 (2006).
- 319 [14] A. Acrivos and T. D. Taylor, “Heat and mass transfer from single spheres in Stokes flow,”
320 *Phys. Fluids* **5**, 387–394 (1962).
- 321 [15] M. Abramowitz and I. A. Stegun, *Handbook of Mathematical Functions*, 3rd ed. (Dover, New
322 York, NY, 1965).
- 323 [16] E. J. Hinch, *Perturbation Methods* (Cambridge University Press, Cambridge, 1991).
- 324 [17] D. G. Crowdy, “Exact solutions for cylindrical slip–stick Janus swimmers in Stokes flow,” *J.*

325 Fluid Mech. **719**, R2 (2013).

326 [18] D. G. Crowdy, “Solving problems in multiply connected domains,” in *NSF–CBMS Regional*
327 *Conference Series in Applied Mathematics* (SIAM, 2020).

328 [19] J. W. Brown and R. V. Churchill, *Complex Variables and Applications* (McGraw-Hill New
329 York, 2003).